Published online 7 July 2017

Nucleic Acids Research, 2017, Vol. 45, No. 17 ***9917–9930***
doi: 10.1093/nar/gkx579

HMGN1 and 2 remodel core and linker histone tail domains within chromatin

Kevin J. Murphy[1], Amber R. Cutter[1], He Fang[1], Yuri V. Postnikov[2], Michael Bustin[2] and Jeffrey J. Hayes[1,*]

[1]Department of Biochemistry and Biophysics, University of Rochester Medical Center, 601 Elmwood Ave, Rochester, NY 14642, USA and [2]Protein Section, Laboratory of Metabolism, Center for Cancer Research, National Cancer Institute, National Institutes of Health, Bethesda, MD 20892, USA

Received May 18, 2017; Revised June 13, 2017; Editorial Decision June 23, 2017; Accepted June 28, 2017

ABSTRACT

The structure of the nucleosome, the basic building block of the chromatin fiber, plays a key role in epigenetic regulatory processes that affect DNA-dependent processes in the context of chromatin. Members of the HMGN family of proteins bind specifically to nucleosomes and affect chromatin structure and function, including transcription and DNA repair. To better understand the mechanisms by which HMGN 1 and 2 alter chromatin, we analyzed their effect on the organization of histone tails and linker histone H1 in nucleosomes. We find that HMGNs counteract linker histone (H1)-dependent stabilization of higher order 'tertiary' chromatin structures but do not alter the intrinsic ability of nucleosome arrays to undergo salt-induced compaction and self-association. Surprisingly, HMGNs do not displace H1s from nucleosomes; rather these proteins bind nucleosomes simultaneously with H1s without disturbing specific contacts between the H1 globular domain and nucleosomal DNA. However, HMGNs do alter the nucleosome-dependent condensation of the linker histone C-terminal domain, which is critical for stabilizing higher-order chromatin structures. Moreover, HMGNs affect the interactions of the core histone tail domains with nucleosomal DNA, redirecting the tails to more interior positions within the nucleosome. Our studies provide new insights into the molecular mechanisms whereby HMGNs affect chromatin structure.

INTRODUCTION

In eukaryotic cells DNA is packaged into chromatin, a dynamic structure consisting of genomic DNA, histones and non-histone proteins. The basic repeating unit of chromatin, the nucleosome core, is composed of ∼147 bp of DNA wrapped around an octamer of histone proteins. Nucleosome cores are connected via linker DNA to form structures resembling beads on a string (hereafter referred to as arrays), which are further organized and folded into chromatin secondary structures such as chromatin fibers and ultimately into higher order structures that are less well understood (1,2). Chromatin compaction affects the ability of regulatory factors such as DNA binding proteins or histone modifying enzymes, to interact with their specific binding sites. Thus, gene expression and other processes that involve genomic DNA alleviate this impediment via ATP-dependent chromatin remodeling mechanisms, acetylation and other post-translational modifications of the core histones, incorporation of histone variants and the directed binding of chromatin architectural factors such as members of the HMGN protein family.

The binding of linker histone (H1) increases the propensity of nucleosome arrays to undergo folding into chromatin fibers and higher-order chromatin structures (2–4). Nucleosome structure-specific binding of linker histones is directed by the linker histone globular domain, which binds within a pocket formed by the exiting/entering DNA strands and the central superhelical wrap within the nucleosome (5–8), while the highly basic H1 C-terminal domain (CTD) provides DNA charge neutralization and is required to condense chromatin into higher-order structures (9–11). The H1 CTD is enriched in Lys, Pro, Ser, Ala and Val residues, consistent with the amino acid composition of an intrinsically disordered domain, and upon binding to nucleosomes undergoes a condensation consistent with adoption of a defined structure, or an ensemble of structures (12–14). Importantly, the H1 CTD structure is dependent on chromatin condensation state and linker DNA conformation (15).

HMGNs are the only nuclear proteins known to bind in a structure-specific manner to the 147-bp nucleosome core particle (NCP), the basic building block of chromatin (16,17). Nucleosome-specific binding is due to an ∼20 amino acid conserved nucleosome-binding domain (NBD), which is enriched in positively charged residues and

*To whom correspondence should be addressed. Tel: +1 585 273 4887; Fax: +585 271 2683; Email: Jeffrey_Hayes@urmc.rochester.edu

contains the invariant core sequence RRSARLSA (18,19). Structural studies show that the NBD core sequence anchors HMGNs to the nucleosome via interactions with the H2A/H2B acidic patch on the histone protein surface of the nucleosome, while the N-terminal portion of the NBD interacts with DNA near the periphery of the dyad axis of nucleosome core (20,21). In addition, footprinting, and chemical crosslinking analyses show that HMGN1/2 interact with both the H3 tail and DNA near the dyad axis of the nucleosome (22,23). Once bound to nucleosomes, HMGNs impact chromatin through a less conserved regulatory domain, which is enriched in negatively charged residues (24,25). This domain functions in opposition of compaction of the chromatin fiber to promote several DNA-dependent nuclear processes such as transcription, DNA replication and DNA repair, as exemplified by the archetypal members of this family, HMGN1 and HMGN2 (formerly HMGN14 and HMGN17, respectively) (26–28).

The close proximity of HMGN and the H1 globular domain (GH1) near the nucleosome dyad combined with their opposing functions on chromatin (reviewed in (29)), lead to the hypothesis that HMGN proteins disrupt the H1-mediated stabilization of condensed chromatin by competing for binding at the entry/exit site of DNA on the nucleosome. Indeed, elevation of either HMGN1 or HMGN2 levels increases the mobility of H1 in live cells as detected by fluorescence recovery after photobleaching (FRAP) experiments (30). Moreover, HMGN1 enhances transcription on SV40 minichromosomes (MCs) in an H1 dependent manner, and also alters the sedimentation profile of H1-containing MCs (31). Interestingly, H1 is found to be still associated with these MCs even after the addition of HMGN1. In MEFs, the mobility of H1-GFP in euchromatin is increased after microinjection of HMGN1; however, the mobility of the more 'stably bound' H1 in heterochromatin was mostly unaffected by HMGN1 addition (30). Moreover, HMGN1 binds to isolated nucleosomes and chromatin containing H1 and *vice versa* (16,32), each apparently interacting with non-overlapping sites on the nucleosome DNA (20,33). Thus, HMGNs may alter H1 interactions and stabilization of chromatin structure via a mechanism other than displacement of H1 from canonical nucleosome binding sites.

In vivo, the HMGN:nucleosome ratio (∼1:100) is significantly less than that for H1, which averages ∼1 H1 per nucleosome (34), however, HMGN1 may be enriched at specific genomic regions where the local concentration is significantly higher (35–37). *In vitro* experiments using nucleosome arrays saturated with HMGN proteins have provided key insights into the mechanism by which these factors open chromatin structure. Importantly, HMGN1 has minimal effects on the structure and salt-dependent folding of nucleosome arrays lacking linker histones (32,38,39). Moreover, while HMGN1 does not alter H1-dependent folding, the HMGN5 variant, which contains a long negatively charged CTD, does reduce the H5-dependent folding of arrays into secondary chromatin structures, (39). Generation of higher order chromatin structure involves both folding of nucleosome arrays into secondary chromatin structures such as the 30 nm chromatin fiber, as well as self-association of arrays into higher order tertiary chromatin structures (2,3), both of which impinge on DNA accessibility. HMGN5's long and negatively charged CTD interacts directly with the CTD of linker histones and reduces the H1-dependent formation of chromatin tertiary structures (39). However, whether HMGN1 or HMGN2 counteracts H1-dependent stabilization of tertiary chromatin structures remains unclear.

To shed light on the mechanism by which HMGN1 and 2 affect the chromatin-condensing activity of H1, we investigated the effects of HMGN binding on linker histone and histone tail interactions within nucleosomes and nucleosome arrays, *in vitro*. We find that HMGN1 diminishes the extent to which H1 stabilizes higher order oligomeric chromatin structures, *in vitro*. Significantly, we find that either HMGN1 or HMGN2 can bind simultaneously with H1 to nucleosomes to form an H1–HMGN1–nucleosome ternary complex that retains the native interactions of the GH1. Using Förster Resonance Energy Transfer (FRET) we discovered that HMGN1 alters the nucleosome-dependent structure of the H1-CTD, as well as directly affecting interactions of the core histone tail domains with nucleosome DNA.

MATERIALS AND METHODS

Reconstitution and purification of nucleosomes and oligonucleosome arrays

Radiolabeled 147, 149, 169 and 217 bp DNA fragments containing a centrally located 601 positioning sequence were generated by polymerase chain reaction (PCR) using pCP1024 as template (40) the following primers: 147: FOR 5′-ACAGGATGTATATATCTGACACG-3′ and REV 5′-CTGGAGAATCCCGGTG-3′, 149: FOR 5′-CACAGGATGTATATATCTGAC-3′ and REV 5′-CCTGGAGAATCCCGGTGCCG-3′, 169: FOR 5′-TCAATACATGCACAGGATGTATATATC-3′ and REV 5′-ACGCGGCCGCCC TGGAGAATCC-3′, 217: FOR 5′-GACTGGCACCGGCAAGG-3′ and REV 5′-CATCCCTTATGTGATGGACCC-3′. Primers (0.5 μg) were radiolabeled prior to PCR by incubation with [γ-32P]-ATP and polynucleotide kinase in recommended buffer (New England Biolabs). PCR products were purified by preparative gel electrophoresis, precipitated, resuspended in TE (10 mM Tris–HCl, pH 8.0, 1 mM EDTA) and stored at 4°C. Nucleosomes were reconstituted by standard salt dialysis method conditions and were empirically optimized by independent adjustment of input recombinant H3/H4 from *Xenopus laevis*, and H2A/H2B purified from chicken erythrocytes to maximize generation of mononucleosome species as described (41). Following reconstitution, nucleosomes were purified by sucrose gradient sedimentation and fractions containing radiolabeled 601 containing nucleosomes and lacking detectable carrier DNA were stored at 4°C for further use.

DNA fragments containing 12 tandemly repeated segments of the '601' nucleosome-positioning sequence was prepared from p207–12sub601 plasmid and reconstituted as described (42). Reconstitution conditions were empirically optimized by independent adjustment of input histone octamers to maximize generation of properly saturated 12mer arrays. Typically, 200 μl reconstitutions contained ∼8 μg each of H3/H4 tetramer and H2A/H2B dimer,

and 15 μg of 12mer array DNA in TE buffer containing 2M NaCl and 5 mM dithiothreitol (DTT). Following reconstitution, the saturation of arrays was determined by $MgCl_2$-dependent self-association assays (42). Arrays with an $MgCl_2$50 ($MgCl_2$ level at which 50% remain in solution) of ∼ 2.5 mM $MgCl_2$ were considered properly saturated.

Self-association of nucleosomal arrays containing HMGN1 and linker histone

Recombinant human HMGN1 and 2 were expressed and purified as in (43) and recombinant *Xenopus* H1.0 was prepared as described (14). Arrays (nucleosome concentration 0.24 μM) were prepared in 1× binding buffer (5% glycerol, 0.15 mg/ml bovine serum albumin (BSA), 0.1 mM ethylenediaminetetraacetic acid (EDTA), 10 mM Tris–HCl 8.0, 50 mM NaCl) with either HMGN1, H1 or both in amounts described in the figure legends and incubated at room temperature for 15 min. Typically, 10 μl of the binding solution was distributed to fresh tubes containing 10 μl 2× $MgCl_2$ in the same buffer to generate final concentrations of 0–10 mM $MgCl_2$ as noted in the figure legends, and incubated at RT for 10 min. Samples were centrifuged at 12 500 × *g* in a microfuge for 10 min then 10 μl of supernatant was removed and mixed with sodium dodecyl sulphate (SDS) loading buffer (1 × 5% glycerol, 0.2% SDS, 0.02% xylene cyanol, 0.02% bromophenol blue in TE) and DNA visualized after electrophoresis on 0.02% SDS and 0.8% agarose gels run at 110 V for 45 min, staining with ethidium bromide and UV exposure. Bio-Rad Image Lab software was used for quantitation relative to arrays in binding buffer alone at 0 mM $MgCl_2$.

HMGN/H1 nucleosome binding assays

Typically binding reactions contained ∼1 nM of gradient purified nucleosomes in 10 μl binding buffer (50 mM NaCl, 10 mM Tris–HCl pH 8.0, 1 mM EDTA, 0.15 mg/ml BSA and 5% glycerol). Proteins in dilution buffer (10 mM Tris–HCl pH 8.0, 1 mM EDTA, 0.1 mg/ml BSA and 5% glycerol) were added sequentially to nucleosomes to generate the concentrations listed in the figure legends, incubated at 4°C for 20 min and samples loaded onto native 0.7% low electroendosmosis agarose (Spectrum) or 5% polyacrylamide gels in 0.5× TBE (45 mM Tris-Borate, pH 8.3, 1 mM EDTA) run at 4°C. The latency associated nuclear antigen virus (LANA) and a control peptide in which residues 8-10 are substituted with alanine (LRS) and is unable to bind to nucleosome acidic patch (44,45) were added to the nucleosomes before addition of HMGNs in the amounts listed in the figure legends. Gels were run at 4°C at 120 V for 3 h, dried and autoradiographed. H1 crosslinking reactions were performed by incubating 1nM 217 bp nucleosomes in binding buffer (10 mM Tris–HCl pH 8.0, 50 mM NaCl, 1 mM EDTA, 0.15 mg/ml BSA, 5% glycerol), with azidophenacyl bromide (APB)-modified H1 G101C or S66C (H1 G101C-APB or H1 S66C-APB) prepared as in Bednar *et al.*, (8) (final concentrations as listed in legend) for 20 min at 4°C. Half of each reaction was directly loaded onto a 0.7% agarose, 0.5× TBE nucleoprotein gel to track formation of H1–nucleosome complexes. The remaining half was UV irradiated at 365 nm for 90 s, SDS-loading buffer was subsequently added and samples were incubated at 37°C for 10 min before loading onto a 0.8% agarose/0.02% SDS-agarose gel. The concentration of H1 S66C-APB or G101C-APB required for maximum formation of the 1:1 H1–nucleosome complex (∼2 nM) was empirically determined and was used for the competition experiments. H1 S66C-APB or G101C-APB was added to 217 bp nucleosomes in binding buffer and incubated at 4°C. After 10 min, 1 nM H1 bound-nucleosome were removed and mixed with either HMGN1, HMGN2 or WT H1 to generate the concentrations listed in legend. Samples were incubated for an additional 20 min at 4°C, subjected to UV irradiation and run on a 0.8% SDS-agarose gel as above to assess formation of crosslinked species.

H3 and H4 tail crosslink mapping

Recombinant *Xenopus* H3 C110A (henceforth referred to as H3), H3 T6C, H3 A14C, H4, H4 G2C and H4 L10C were prepared as described (41) and tetramers generated combining cysteine substitution mutants with the appropriate WT protein. The H3/H4 tetramers were reduced with DTT, modified with APB as described (41) and nucleosomes reconstituted with H2A/H2B 217 bp DNA fragments containing a single radioactive end-label, as described above. Nucleosomes (∼25 K cpm, ∼100 fmol) containing APB-modified proteins were incubated in binding buffer (50 mM NaCl, 10 mM Tris–HCl pH 8.0, 1 mM EDTA, 0.15 mg/ml BSA and 5% glycerol), in the presence or absence of 0.5 pmol HMGN1 or HMNG2 in a total volume of 120 μl at 4°C. Nucleosomes were UV irradiated for 30–90 s, ethanol precipitated and resuspended in dH_2O, treated with 1M piperidine at 90°C for 30 min, dried and analyzed on 5% acrylamide, 8M Urea denaturing sequencing gels. Gels were dried and analyzed by phosphorimager. Two to three independent determinations were performed for each crosslinking configuration.

HMGN/H1 nucleosome crosslink mapping

The concentration of H1 S66C-APB or G101C-APB required for maximum formation of the 1:1 H1–nucleosome complex was empirically determined as above. H1 S66C-APB or G101C-APB was added to 217 bp nucleosomes in binding buffer and incubated at 4°C. After 10 min, HMGN2 was added and samples were incubated for an additional 20 min at 4°C. A portion of binding reaction was analyzed on native 0.7% agarose gels, the remaining reaction subjected to UV irradiation at 365 nm 90 s and a portion run on a 0.8% agarose-SDS gel to assess formation of crosslinked species. Remainder of crosslinked material was mapped by piperidine base elimination and sequencing gel analysis as in Bednar *et al.*, (8). Two to three independent determinations were performed for each crosslinking configuration. Crosslinks were mapped onto models generated from the 1KX5 structure (46), or a model generated by combining histones from the 1KX5 structure with 197 bp DNA and GH1 from Complex A in ref (5) by iterative alignment of core DNA strands.

H1-CTD FRET and HMGN1 binding

FRET analysis was performed with 207 bp nucleosomes containing 601 DNA and Cy3/Cy5 labeled *Xenopus* H1.0 double mutant G101C/K195C, prepared as described (14). Binding reactions containing 1.8 nM nucleosomes were incubated with 1.8 nM of labeled H1G101C/K195C, and either 0, 0.9 or 1.8 nM HMGN1 in a final volume of 150 μl in binding buffer (10 mM Tris–HCl pH 8.0, 1 mM EDTA, 50 mM NaCl and 0.3 mg/ml BSA). Emission spectra were recorded with excitation at 515 and 610 nm wavelengths on a Horiba Jovin Yvon FluoroMax-4 Spectrofluorometer with 4 nm slit widths in both channels and a KV 550-nm cut-off filter in the emission channel. Spectra were recorded in the absence or presence of HMGN1. FRET spectra were recorded and analyzed as described (15).

RESULTS

The mechanism by which HMGN1 and HMGN2 alter chromatin architecture remains unclear (25,29,47). To determine whether HMGN1 or HMGN2 alters formation of higher order tertiary chromatin structures, we employed self-association assays, which assess inter-fiber interactions in chromatin (2,48,49). Nucleosome arrays reconstituted with core histones and a 2.5 kb DNA template containing 12 × 207 bp tandem repeats of the 601 nucleosome positioning sequence, exhibited 50% self-association in 2–3 mM $MgCl_2$ in low-salt buffer (0 mM NaCl) (results not shown), as expected for arrays fully saturated with histones (42,48). However, in H1/HMGN binding buffer containing 50 mM NaCl the Mg50 ($MgCl_2$ concentration at which 50% of arrays undergo self-association) of the arrays increases to ∼4–5 mM $MgCl_2$. (Figure 1A), consistent with published results (38), HMGN1 added to the arrays in the absence of H1 had no effect on array self-association when present at a ratio of 2 HMGN1s per nucleosome (Figure 1A). As expected, when the arrays were first incubated with H1 at a stoichiometry of 1 per nucleosome, we observed self-association at much lower concentrations of $MgCl_2$ (Figure 1B). Importantly, in contrast to the absence of effect on H1-lacking arrays, the addition of either one or two molecules of HMGN1 per nucleosome significantly diminished self-association of H1-bound arrays (Figure 1C). The effect of HMGN1 on H1-facilitated formation of self-associated arrays is most prominent between ∼1.5 and 2.5 mM $MgCl_2$ as arrays still achieve complete self-association at higher concentrations of $MgCl_2$. Similar results were obtained for HMGN2 (data not shown).

To understand how HMGN1 and 2 might affect H1-dependent array self-association, we first investigated how these proteins interact with 169 bp nucleosomes containing H1. As the majority of studies to date have utilized 147 bp native nucleosome CPs generated by micrococcal nuclease digestion, which lack linker DNA but contain the endogenous complement of histone subtypes, post-translational modifications and random DNA sequences (25,50), we confirmed that HMGN1 and 2 interact in a similar manner with reconstituted, 169 bp nucleosomes containing recombinant histone proteins and linker DNA, which is necessary for H1 binding. HMGN1 and 2 bound reconstituted 147 bp nucleosome cores containing the Widom '601' sequence (capable of positioning the nucleosome at a single translational position on the DNA) with the prototypical 2:1 stoichiometry (Figure 2A and Supplementary Figure S1). Likewise, incubation of HMGN1 or 2 with reconstituted 169 bp nucleosomes exhibited apparent stepwise association of one and then two molecules of HMGN (Figure 2B and C). Thus HMGN1 and 2 bind to reconstituted nucleosomes containing linker DNA in manner identical to that previously described for native NCPs (38,50)

Methyl-TROSY nuclear magnetic resonance spectroscopy revealed a specific interaction between the highly conserved HMGN NBD and an H2A.H2B acidic patch on the nucleosomal surface (21). It was previously shown that a 22-residue peptide from the LANA, which binds to the acidic patch with high affinity (51,52), can compete with

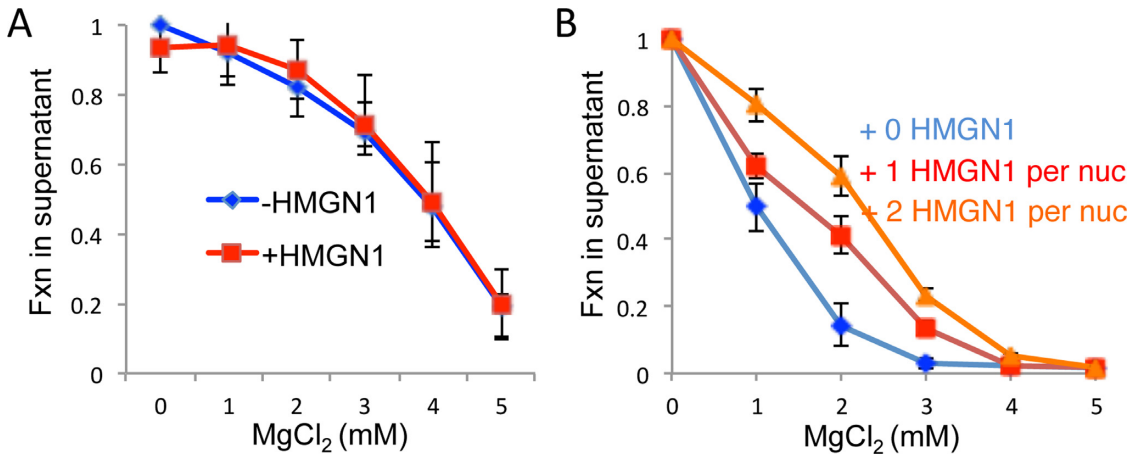

Figure 1. HMGN1 reduces the H1-dependent stabilization of nucleosome array self-association. Nucleosomes arrays were prepared and the fraction of the sample remaining soluble in the presence of increasing $MgCl_2$ determined as described in the 'Materials and Methods' section. (**A**) $MgCl_2$-dependent self-association of 12-mer arrays in 50 mM NaCl binding buffer is unaffected by HMGN1, at a ratio of 2 HMGN per nucleosome. (**B**) The stimulation of H1 array oligomerization is partially abrogated by HMGN1, at ratios of 1 and 2 HMGN1s per nucleosome. Note that H1 significantly increases oligomerization of arrays into higher-order chromatin structures at a ratio of 1 H1 per nucleosome in 50 mM NaCl binding buffer (3). Errors reported are ±standard error, $N = 3$.

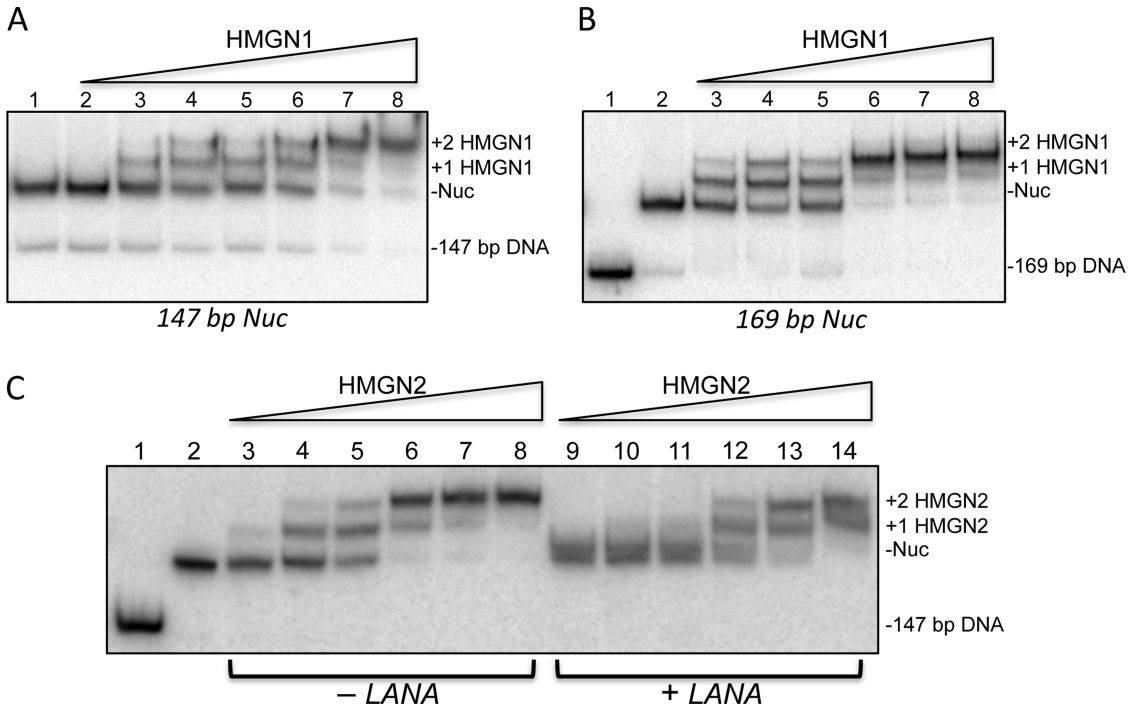

Figure 2. Mobility shift assays showing specific binding of HMGN1 and 2 to nucleosomes (169 bp) and nucleosome core particles (NCPs) (147 bp). (**A**) HMGN1 binding to 147 bp NCPs. Lanes 1–8 show nucleosomes (2 nM) incubated with 0, 0.1, 0.2, 0.5, 1, 2, 4 and 20 nM HMGN1, respectively. (**B**) HMGN1 binding to 169 bp nucleosomes. Lane 1, nucleosomes with sodium dodecyl sulphate (SDS) loading buffer, lanes 2–8, nucleosomes (2 nM) with 0, 0.2, 0.5, 1, 2, 4, 8, 15, nM HMGN1, respectively. (**C**) HMGN2 binding to 2 nM NCPs (147 bp) is competed by LANA peptide. Lanes 1 and 2 contain 147 bp nucleosomes in the presence and absence of SDS, respectively. Lanes 3–8 and 9–14 contain 0.5, 1, 2, 4, 8 and 15 nM HMGN2, respectively. LANA peptide is present at a concentration of 0.1 μM in samples run in lanes 9–14. Note small shift in nucleosome position due to LANA binding. All analyses were on native 5% acrylamide-0.5× TBE gels. Note that LANA binding directly to the nucleosome causes a small shift in the nucleosome band.

the H4 tail domain, which also binds to the acidic pocket (45). Likewise, we find that the LANA peptide partially competed with HMGN2 for binding to the nucleosome, while an altered peptide (LRS) with the same charge but unable to bind to the nucleosome acidic pocket (51) did not compete (Figure 2C, compare lanes 3 and 4 to 9 and 10, and Supplementary Figure S1). Moreover, we find that LANA similarly reduced HMGN1 binding to nucleosomes (Supplementary Figure S2). Thus, interaction with the acidic pocket on the nucleosome's protein surface appears to be a common feature of both HMGN1 and 2 binding to nucleosomes, a finding that agrees with the sequence conservation in NBD of this protein family (53).

We next employed native gel-shift assays to determine whether HMGNs function by excluding or competing with H1 for binding to nucleosomes. As previously observed (14), H1 binds to nucleosomes to form a complex with a 1:1 stoichiometry seen as a discrete band on native gels (Figure 3A, lane 3). Similarly, nucleosomes incubated with HMGN1 resulted in the generation of slower-migrating species, consistent with binding of one, and then two molecules of HMGN1 to each nucleosome (Figure 3A, lanes 4–6). Introduction of the same amount of HMGN1 to H1-bound nucleosomes did not cause a diminution of the H1–nucleosome band; rather, a supershifted band was observed, consistent with simultaneous binding of HMGN1 and H1 to the same nucleosome (Figure 3A, lanes 7–9). Likewise, reversing the order of addition, such that H1

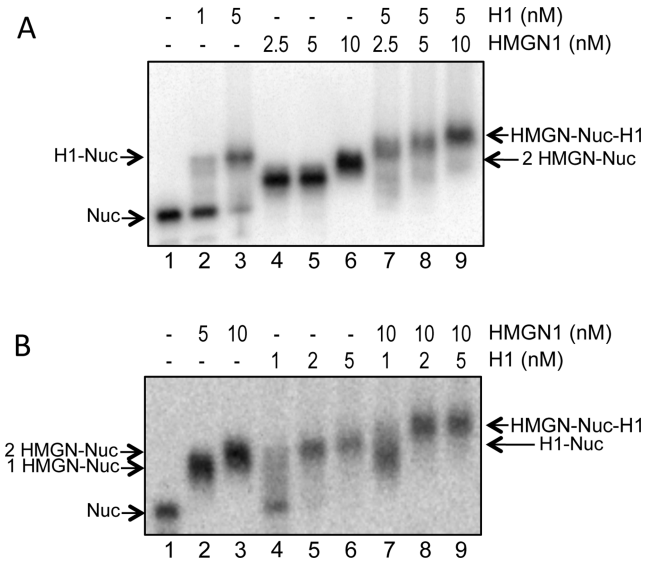

Figure 3. HMGN1 and H1 bind simultaneously to a nucleosome. (**A**) HMGN1 supershifts H1-bound nucleosomes. Nucleosomes (~2 nM) were incubated with either 0, 1 or 5 nM H1 (lanes 1–3), or 2.5, 5 or 10 nM HMGN1 (lanes 4–6). Lanes 7–9 show nucleosomes first incubated with 5 nM H1, then 2.5, 5 or 10 nM HMGN1. (**B**) H1 supershifts HMGN1-bound nucleosomes. Experiment was carried out as in (A) except that HMGN1 was incubated with nucleosomes prior to addition of H1 in lanes 7–9. Shown are autoradiographs of native 0.7% agarose nucleoprotein gels.

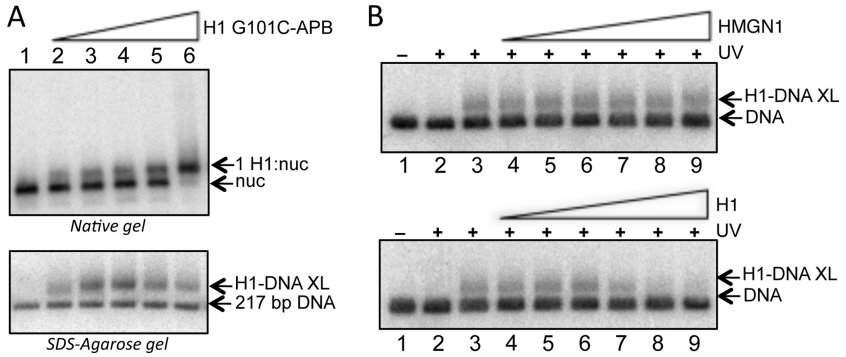

Figure 4. HMGN1 does not displace H1 from nucleosomes. (**A**) H1 G101C-APB binds to nucleosomes as indicated by mobility shift on native gels (top) and formation of a covalently crosslinked species (bottom). Nucleosomes (5 nM) assembled with radiolabeled 217 bp DNA templates were incubated with increasing amounts of H1 G101C-APB then half of each sample loaded directly onto the native gel (top) and half irradiated with UV light to induce crosslinking, and loaded onto an SDS-agarose gel (bottom). Lane 1, nucleosome alone, lanes 2–6 contain ∼0.5, 1, 1.5, 3 and 6 nM H1 G101C-APB, respectively. (**B**) HMGN1 does not displace H1–DNA interactions within the nucleosome. Nucleosomes (5 nM) were incubated with H1 G101C-APB (3 nM), then challenged with increasing HMGN1 or unmodified H1, irradiated and crosslinked H1–DNA products separated on SDS-agarose gels. Lanes 1 and 2, nucleosome alone, lanes 3–9, nucleosomes incubated with H1 G101C-APB (3 nM) and 0, 0.1, 0.4, 2, 10, 50 and 100 nM HMGN1 (top) or unmodified H1 (bottom). Samples were irradiated as indicated (UV). Gels were dried and phosphorimaged.

was added to samples containing HMGN1–nucleosome complexes resulted in a similar super-shifted complex that migrated slower than nucleosomes associated with either HMGN1 or H1 alone (Figure 3B, compare lanes 3, 6 and 9). These results indicate that both H1 and HMGN1 (and 2, see below) can bind to the same nucleosome, and are consistent with previous results showing HMGN2 and H1 within mononucleosome species generated by micrococcal nuclease digestion (16).

The GH1 has been shown to interact with nucleosomes near the dyad axis, where the linker DNA enters/exits the structure. Similarly, hydroxyl radical footprinting indicates that HMGNs also interact with the nucleosomal DNA in the same vicinity (7,20). To substantiate the above results, and determine whether nucleosome-specific binding of the GH1 remains intact upon HMGN association, we employed a crosslinking assay to monitor interactions between the GH1 and nucleosomes in solution in either the presence or absence of HMGNs. An H1 containing a single cysteine substitution (H1 G101C, see 'Materials and Methods' section and (8) was modified with 4-azidophenacylbromide (APB), a photo-inducible crosslinking agent. Nucleosomes were incubated in binding buffer with increasing amounts of H1 G101C-APB, half of the sample was loaded onto a native 0.7% agarose gel to confirm binding via gel-shift assay, while the other half was irradiated with UV light, then mixed with SDS loading buffer and run on a 0.8% SDS-agarose gel to observe covalently crosslinked products. With increasing amounts of H1, a discrete slower migrating species was observed on the native gel, indicating formation of an H1–nucleosome complex (Figure 4A, top), as observed with unmodified H1 (see Figure 3). Importantly, a band corresponding to a crosslinked H1-DNA species appeared on the SDS-agarose gel, commensurate with the appearance of the H1–nucleosome complex (Figure 4A, bottom). Thus, the formation of the crosslinked species is indicative of H1 binding to the nucleosome in solution. To assay for potential HMGN1 disruption of H1–nucleosome interactions, nucleosomes were incubated H1 G101C-APB at a final concentration of ∼3 nM, where binding to nucleosomes was observed to be sub-stoichiometric, then increasing amounts of HMGN1 were added to the samples, prior to crosslinking. At levels of HMGN1 corresponding to two molecules per nucleosome, we observed that the extent of H1 G101C-APB crosslinking is unaffected (Figure 4B, top, lane 7). In fact, even when HMGN1 is present in ∼20-fold molar excess over the H1–nucleosome complex (lane 9), H1G101C-APB the crosslinked band is still at ∼80% that in the absence of HMGN1. Similar results were obtained with HMGN2, using H1 G101C-APB (Supplementary Figure S3) and also by probing a second contact between the GH1 and nucleosomal DNA, using APB-modified H1 S66C (Supplementary Figure S4). As a positive control for competition of H1G101C-APB binding to the nucleosome, unmodified WT H1 was added in an identical fashion as HMGN1. Addition of H1 resulted in a significant decrease of H1G101C-APB crosslinking, even at levels only a few-fold in excess of the H1–nucleosome complex (Figure 4B, bottom, lane 7). Thus neither the presence of HMGN 1 nor HMGN2 at concentrations well above that necessary for nucleosome binding appear to disrupt binding of GH1 to the nucleosome.

Next, we mapped sites of crosslinking to verify that the specific location of globular domain interactions with the nucleosomal DNA were not altered upon the binding of HMGNs. Nucleosomes were incubated with either H1 G101C-APB or H1 S66C-APB and generation of super-shifted complexes upon addition HMGN2 confirmed by running a portion of the reaction on native gels (Figure 5A, upper panel). The remainder of the reaction was exposed to UV light to induce formation of crosslinks to DNA; consistent with results reported above, the yield of crosslinks was not affected by binding of HMGN2 (Figure 5A, lower panel). Finally, sites of crosslinking were mapped to single-nucleotide resolution as described (8). Inspection of the denaturing 'sequencing' gels indicates that neither the yield nor position of crosslinks was altered upon binding of HMGN2 to H1–nucleosome complexes (Figure 5B). We

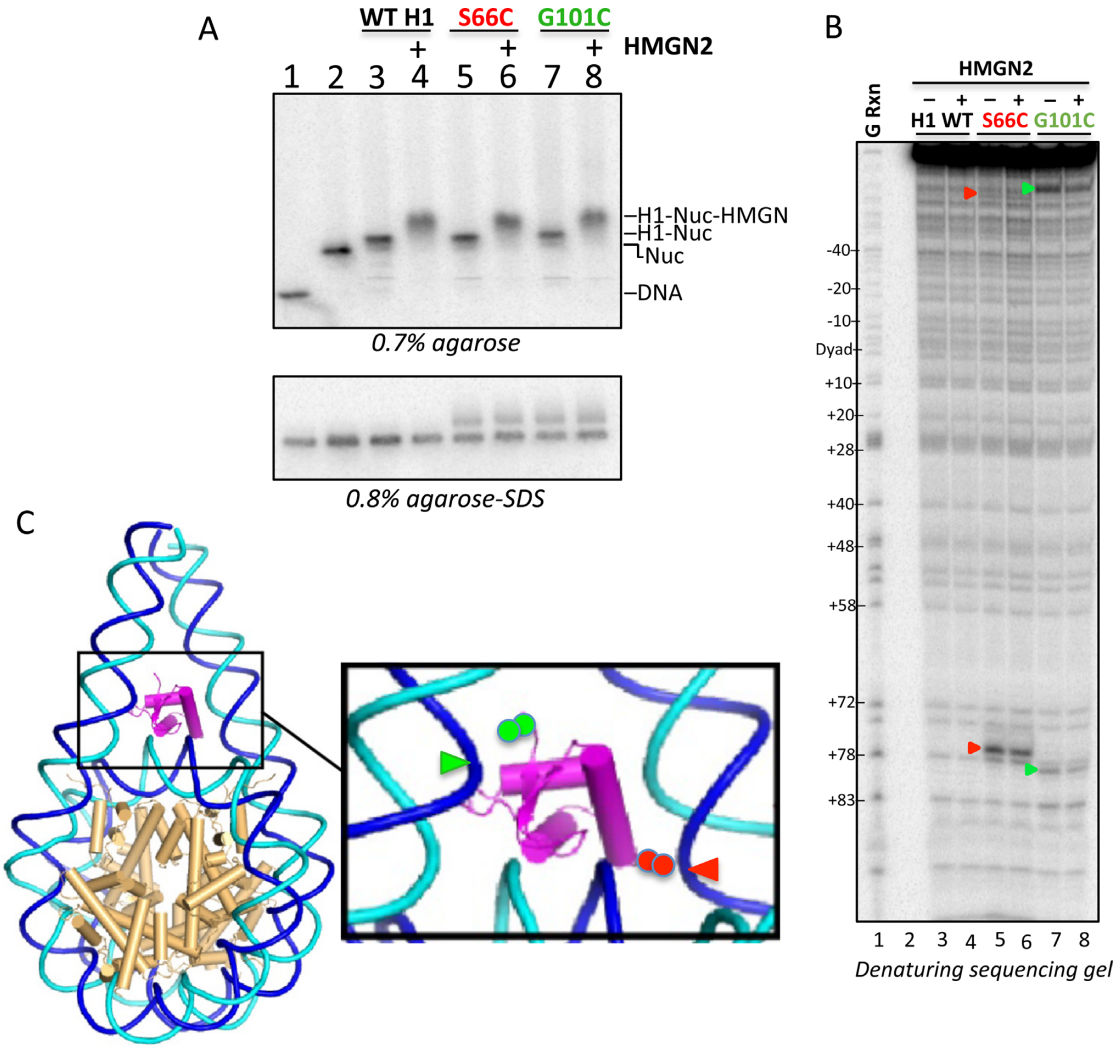

Figure 5. HMGN2 binding does not alter specific interactions of the H1 globular domain (GH1) with nucleosomal DNA. (**A**) Top: colocalization of HMGN2 and H1 on nucleosomes detected by super-shift assay. Lane 1, naked DNA, lanes 2–8 contain nucleosomes (2 nM) in the presence of WT H1 (lanes 3 and 4), H1 S66C-APB (lanes 5 and 6) or H1 G101C-APB (lanes 7 and 8), in the absence (lanes 3, 5 and 7) or presence of 20 nM HMGN2 (lanes 4, 6 and 8, respectively). Bottom: denaturing agarose-SDS gel showing H1 crosslinking to 217 bp nucleosomes in the presence or absence of HMGN2, as indicated. (**B**) Sequencing gel analysis of H1–nucleosomal DNA crosslinks from samples in A mapped by piperidine base elimination cleavage of DNA. Nucleotides crosslinked to H1 S66C-APB and G101C-APB (detected as enhanced band intensity) are indicated by red and green arrowheads, respectively. (**C**) Model of GH1 interactions with nucleosomal linker DNA, positions of modified residues and crosslinked nucleotides mapped in B indicated by red and green filled circles and arrowheads, respectively.

observed that amino acid 101 within the globular domain of H1 was juxtaposed to positions ±79/±80 of nucleosomal DNA and amino acid 66, located on the opposite face of this domain, was juxtaposed to positions ±77 of nucleosomal DNA, consistent with a recent model for how H1 binds to nucleosomes (8) (Figure 5C). In summary, these results indicate that H1 can bind simultaneously to nucleosomes with either HMGN1 or 2, to form an HMGN–nucleosome–H1 complex in which the structure-specific interactions of the GH1 are unaffected.

Since we find that HMGN proteins do not displace H1 from nucleosomes nor alter nucleosome structure-specific interactions of the GH1, we sought to understand how these proteins may otherwise influence linker histones to affect tertiary chromatin structure. Specifically, we tested whether nucleosome-induced folding of the H1 CTD, which has been linked to chromatin condensation (15) is altered by HMGN proteins. We have previously employed FRET to monitor nucleosome-directed folding of the H1 CTD by placing donor/acceptor pairs at opposite ends of the this domain (Figure 6A) (14,15). As reported previously, Cy3/Cy5-modified H1 G101C/K195C exhibits only small amounts of FRET when free in solution (Figure 6B, black trace), consistent with a disordered H1 CTD (14). However, upon binding to nucleosomes, a significant increase in FRET is observed (exemplified by the increased emission peak at ∼670 nm, Figure 6B, dark blue trace), indicative of nucleosome-specific condensation of the CTD and consistent with formation of a defined fold or ensemble of folds within this domain (15). Surprisingly, as HMGN1 was added to H1-bound nucleosomes, we observed an additional increase in the FRET signal, indicating

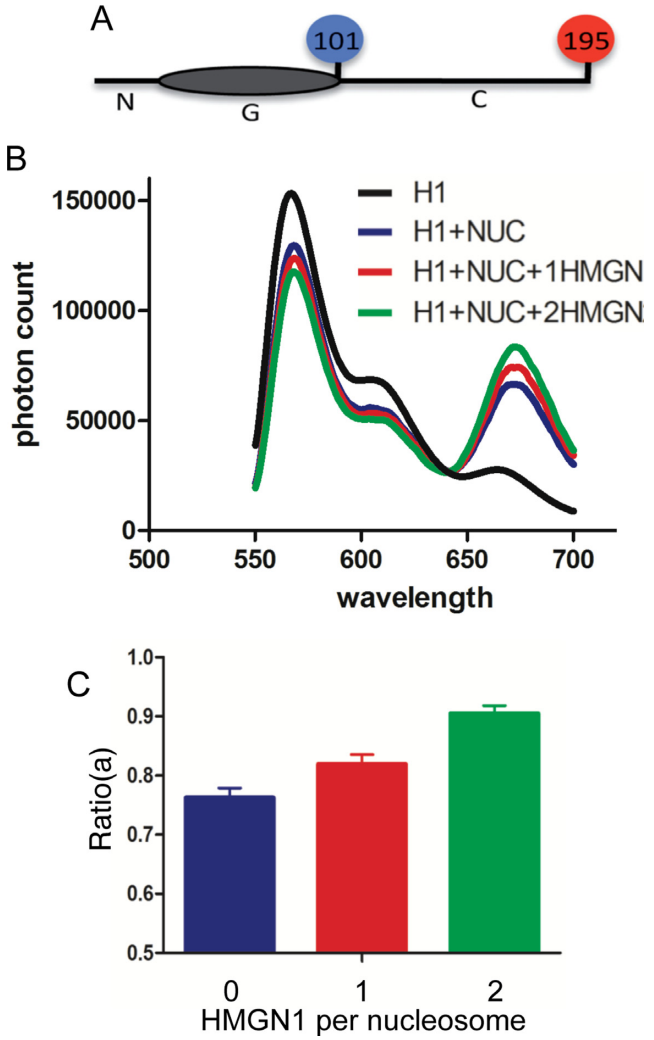

Figure 6. HMGN1 increases condensation of the H1 COOH terminal domain when bound to nucleosomes. (**A**) Schematic showing sites of Cy3 and Cy5 labeling within H1 G101C K195C. N, G and C denote N-terminal, Globular, and C-terminal domains, respectively. (**B**) Emission spectra upon excitation at 515 nm for Cy3/Cy5 labeled H1 G101C K195C in the absence of nucleosome (black line), in a 1:1 complex with nucleosomes alone (blue line) or incubated with 1 (red line) or 2 (green lines) HMGN1 per nucleosome. (**C**) Graph of Ratio(a) measure of FRET efficiency versus HMGN1 per nucleosome. Error bars represent ±1 standard deviation, $N = 3$.

an HMGN1-dependent change H1 CTD structure. Specifically, HMGN1 induced an increase in Ratio(a), a measure of FRET efficiency, from ∼0.76 for the H1–nucleosome complex alone, to ∼0.9 for nucleosomes incubated with 2 HMGN1s per complex (Figure 6C). This result indicates that HMGN1 induces a further transition in H1 CTD structure to a more compact conformation (or ensemble of conformations) when bound to the nucleosome.

In addition to interactions with linker histones, site-directed crosslinking reveals contacts between the N-terminal region of HMGNs and a region spanning residues 20–50 within the N-terminal tail region of H3 in nucleosomes, which may contribute to destabilization of condensed chromatin structures (23). The N-terminal tail domains of H3 and H4 contribute significantly to folding and self-association of nucleosome arrays, and are, in combination, indispensable for this process *in vitro* (54). To assess whether HMGN1 or HMGN2 alters histone tail interactions in chromatin, we examined H3 tail contacts to DNA within nucleosomes using site-specific crosslinking capable of capturing interactions with nucleosomal DNA at single-nucleotide resolution. We first mapped contacts of the H3 tail domain in nucleosomes containing radiolabeled 207 bp 601 DNA fragments and APB-modified H3T6C, wherein the photo-activatable probe is located near the N-terminus of the tail domain. The nucleosomes were irradiated to induce crosslinking in the absence or presence of HMGN1 or HMGN2 and crosslink-specific cleavages of the DNA backbone mapped on denaturing 'sequencing' gels (see 'Materials and Methods' section). We find that nucleosomes containing H3 T6C-APB crosslink to DNA bases positions −77, −72, −64, −14, +23, +62 and +82 (Figure 7A, compare lane 1 (−UV) to lanes 2 and 3 (+UV, and +UV + binding buffer, respectively), base positions indicate distance from the dyad base as in (5)). The majority of crosslinks form a constellation of sites on the side of the nucleosome, near superhelix location (SHL) ±1.5 and ±2.0 (Figure 7B), indicating that the tail, which exits through the superhelical gyres at aligned grooves near SHL ±1.0 must fold back onto the structure, similar to the conformation of one of the two H3 tail domains in the 1KX5 crystal structure of the nucleosome core, in which the tail domains are fully modeled (46) (PDB ID: 1KX5). (Note in this structure, the two H3 N-terminal tail domains adopt distinct conformations.) Importantly, contacts detected at positions −77 and +82 nt from the dyad map to outside the nucleosome core, within the linker DNA (Figure 7B), indicating that the H3 tail can project out from the core when linker DNA is present, as predicted from molecular modeling (55). Fortuitously, the second H3 tail domain in the 1KX5 crystal structure (which lacks linker DNA) extends out from the nucleosome core due to interactions with a neighboring nucleosome core in the crystal lattice (46). This H3 tail conformation aligns well with the mapped contacts at −77 and +82 in a model constructed with linker DNA (5), (Figure 7B). Importantly, binding of HMGN1 or HMGN2 causes similar, specific changes in the crosslinking pattern for the H3 domain as measured by H3 T6C-APB crosslinking (Figure 7A, compare lane 3 (binding buffer alone) to lane 4 (+HMGN1) and lane 5 (+HMGN2)). In general, contacts to the interior nucleosome core DNA are unaffected, while the H3 tail contacts with the linker DNA, as indicated by crosslinks to −77 and +82, are disrupted by binding of HMGNs (Figure 7A, compare lane 3 to lanes 4 (+HMGN1) and lane 5 (+HMGN2) and Figure 7B).

To further investigate tail rearrangements, we performed the crosslinking experiments with an H3 in which the modified residues located more internally within the tail domain. Nucleosomes containing H3 A15C-APB were prepared and crosslinking to DNA analyzed as above. We detected crosslinking to sites clustered near the nucleosome dyad, and the edge of the nucleosome core DNA, near SHL ±0.5, ±6.5 and ±7.0, respectively (Figure 8). Upon binding of HMGN1, crosslinking sites nearest the dyad (SHL ±0.5 and ±7.0, cyan in Figure 8) are reduced or eliminated

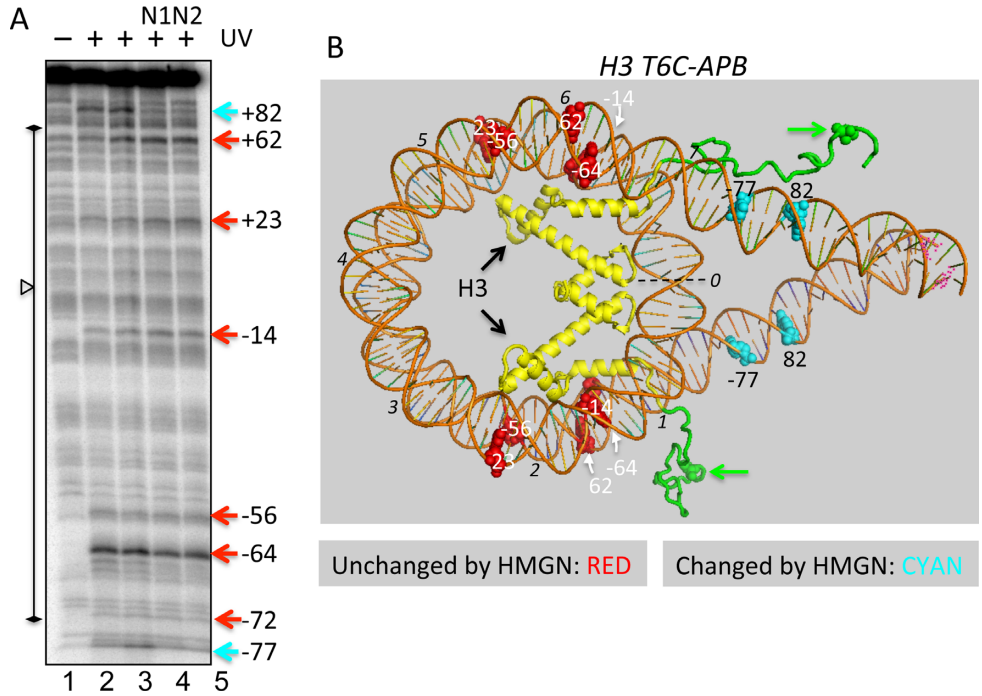

Figure 7. Specific interactions between the H3 N-terminal tail domain and nucleosome DNA are altered by HMGN1 and HMGN2. (**A**) Nucleosomes containing H3 T6C-APB were irradiated with UV light and the sites of crosslinking to the radiolabeled DNA determined by crosslink-specific cleavage of the DNA and analysis of products on denaturing 'sequencing' gels. Lane 1, no UV; lanes 2–5, nucleosomes irradiated with UV light in TE (lane 2), 50 mM NaCl binding buffer (lane 3) or binding buffer with HMGN1 or HMGN2 (lanes 4 and 5, respectively). Shown is a phosphorimage of the gel. Sites of crosslinking are indicated by arrows and numbers, according to distance from dyad base (0), as in (5); sites unaffected or affected by HMGN binding are indicated in red and cyan arrows, respectively. The effect of HMGNs on crosslinking was confirmed by band quantification (Supplementary Table S1). The vertical bar indicates DNA within the nucleosome core region, with the dyad marked by an open triangle. (**B**) Model of H3 N-terminal tail domain crosslinking sites within the nucleosome, showing H3 (yellow) and H3 N-tail residues 1–37 colored green, with site of crosslinker attachment (T6C) indicated by space filling residues and green arrows. All other core histones are omitted for clarity. Sites of crosslinking on the DNA are indicated by space-filling bases, with sites for which crosslinking is unaffected by HMGN association shown in red, while those for which crosslinking is reduced are cyan. Black italic numerals indicate superhelix location (SHL) for the top wrap of DNA in the nucleosome.

while those further away from the dyad (SHL ±6.5) are unperturbed. These results correlate well with those obtained with nucleosomes containing H3 T6C-APB, in which contacts to linker DNA were abrogated by HMGN proteins in favor of more internal sites within the nucleosome (Figure 7).

We also investigated possible effects of HMGN1 on interactions of the H4 tail domain. Nucleosomes containing H4 L10C-APB exhibit strand-specific crosslinking at base positions −16, +16, −26 and +27 (Figure 9A). Mapping of these positions onto a model of the nucleosome indicates that crosslinking is localized to two symmetry-related clusters in each half of the nucleosome at SHL ±1.5 and ±2.5 (Figure 9B). Crosslinks at −26, and +27 form symmetry-related sites near SHL ±2.5, which correspond well to the location of one of the two H4 tail domains in the X-ray crystal structure of a nucleosome core where the core histone tail domains are fully modeled (46). (In this structure, the two H4 N-terminal tail domains adopt distinct conformations, with the terminus of one H4 tail (denoted 'H4' here) occupying the major groove at SHL ±2.5 (Figure 9B and C).) In addition, the remaining crosslinks, at positions −16 and +16, form a second cluster, centered around SHL ±1.5 (Figure 9). This cluster is near the other H4 tail domain in the 1KX5 structure, here indicated as H4' (Figure 9B and D). Interestingly, similar to the effect on H3 tail interactions, binding of HMGN1 greatly reduces H4 L10C-APB crosslinking nearest the dyad (−16 and +16) while the crosslinks further away (−26 and +27) appear largely unperturbed (Figure 9).

DISCUSSION

Our work provides novel insights into the mechanisms by which HMGNs alter chromatin structure to affect various processes that are modulated by chromatin compaction and organization. We find that HMGN1 and 2 reduce the propensity of nucleosome arrays to undergo self-association into higher order chromatin structures, in an H1-dependent manner. Self-association involves long-range inter-fiber interactions that are thought to be crucial to the formation of higher-order chromatin structures of interphase chromosomes (2). Significantly, we find that while HMGN1 and 2 do not directly displace H1 from mononucleosomes or disturb specific GH1 interactions with the nucleosome, these proteins directly alter both core histone tail interactions, and the nucleosome-dependent condensation of the H1 CTD. Thus our data argue that binding of HMGN1 and HMGN2 to nucleosomes leads to rearrangements of core and linker histone tail interactions, leading to a less condensed chromatin structure.

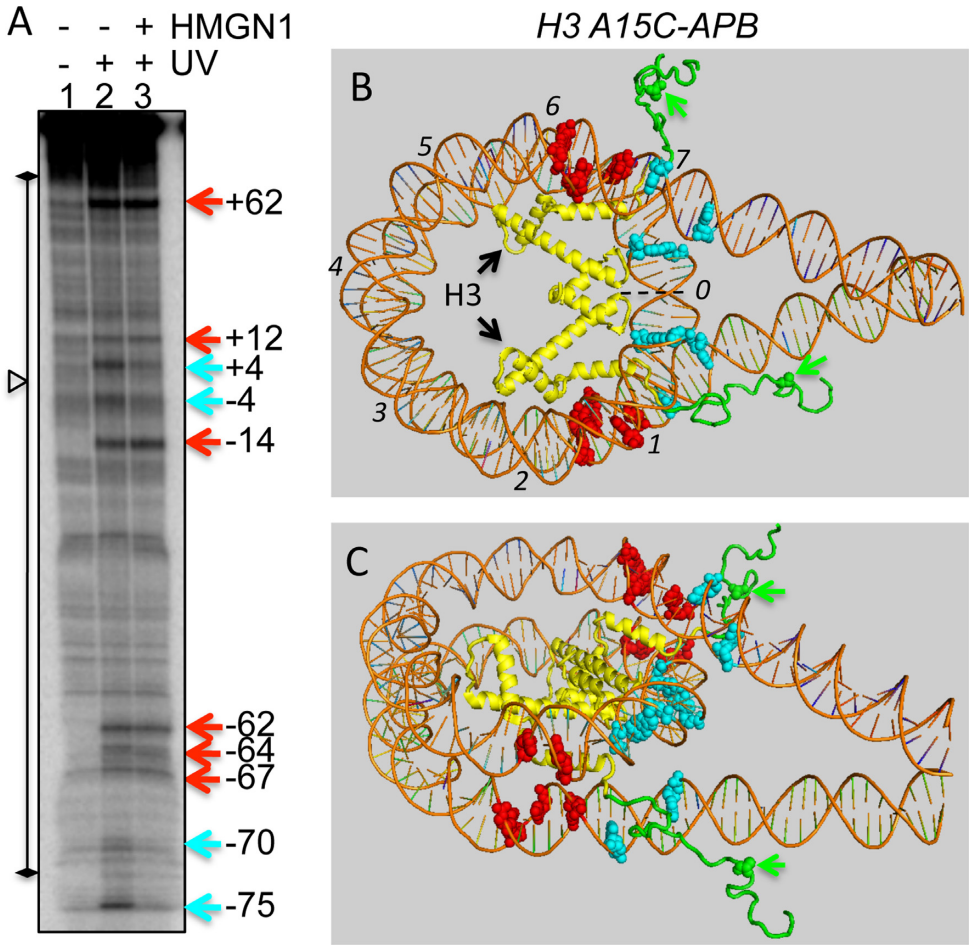

Figure 8. HMGN1 alters crosslinking of an interior position within the H3 tail domain to DNA within the nucleosome. Crosslinking was carried out as in Figure 7 except that the site of APB attachment was located at residue 15 within the H3 tail domain. (**A**) Sequencing gel showing sites of crosslinking for nucleosomes containing H3 A15C-APB. Lane 1, -UV irradiation, lanes 2 and 3, +UV in the absence or presence of HMGN1, respectively. Sites of crosslinking are indicated by arrows; those unaffected by HMGN1 binding are red, those affected by HMGN1 binding are cyan. (**B** and **C**) Models showing top (B) and oblique views (C) of crosslinked bases, with sites unaffected or affected by HMGN1 indicated by red or cyan arrows, respectively. H3 is yellow, with H3 N-tail residues 1–37 colored green and other histones omitted for clarity. Sites of APB attachment indicated by space-filling green residues and green arrows. Other core histones are omitted for clarity.

Linker histones stabilize both folding of nucleosome arrays into chromatin fibers, as well as further condensation via self-association of arrays into chromatin tertiary structures (3). Interestingly, hydrodynamic studies have established that the major HMGN variants, HMGN1 and HMGN2 do not alter folding of nucleosome arrays lacking or containing linker histones H1 into secondary chromatin structures, such as the chromatin fiber (38,39). Here we used well-defined nucleosome arrays to test whether these proteins alter the formation of higher order tertiary chromatin structures, modeled by Mg^{2+}-induced self-association of arrays (2,56). Such structures involve long-range internucleosome interactions mediated by the core histone tail domains, and are stabilized by linker histones (1,45). We found that while HMGN1 and 2 did not alter the propensity of arrays lacking H1 to undergo Mg^{2+}-dependent self-association, they did counteract linker histone-dependent stabilization of higher order self-associated structures (Figure 1). Given the juxtaposition of HMGN and H1 binding sites on the nucleosome surface, it has been suggested that HMGNs may compete for binding to nucleosomes with H1. Indeed, FRAP analyses of living cells indicates that HMGNs reduce the chromatin residence time of H1, especially in the less condensed euchromatin regions (30). However, we find that HMGN1/2 and H1 can simultaneously bind to nucleosomes. In particular, we show that incubation of both proteins at stoichiometric ratios with nucleosomes produces a super-shifted complex that migrates more slowly than either the H1–nucleosome or HMGN1–nucleosome complex and that the formation of this putative ternary structure is independent of order of addition of the proteins (Figure 3). Our results with reconstituted nucleosomes are consistent with a prior study showing that MNase releases mononucleosome species from mammalian cells containing both H1 and HMGNs, and that these proteins can be added back to stripped MNase-generated mononucleosomes to generate a similar super-shifted complex. (16). As gel-shift experiments rely on detection of complexes under non-equilibrium conditions, we additionally used previously described chemical crosslinking to track H1 bind-

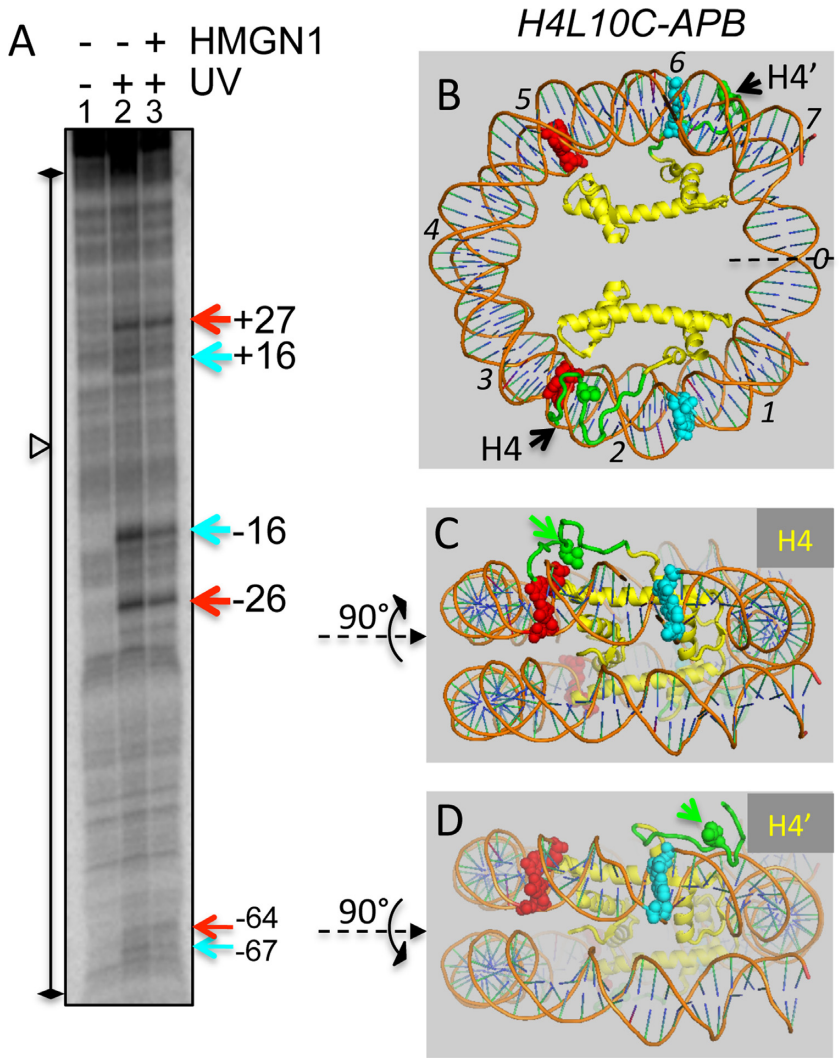

Figure 9. HMGN1 alters crosslinking of the H4 tail domain to DNA within the nucleosome. Crosslinking was carried out as in Figure 7 except that the site of APB attachment was within H4 tail domain. (**A**) Denaturing sequencing gel showing sites of crosslinking for nucleosomes containing H4 L10C-APB. Lane 1, −UV irradiation, lanes 2 and 3, +UV in the absence or presence of HMGN1, respectively. (**B**) Model of nucleosome with view down superhelical axis, with H4 (yellow), H4 N-tail residues 1–21 colored green and site of crosslinker attachment (L10C) indicated by the space-filling residue in the tail domain. Other histones are omitted for clarity. Nucleosome dyad is indicated as a dashed line. Model adapted from 1KX5 structure (46), in which the H4 are fully modeled and have distinct conformations, indicated here as H4 and H4' (black arrows). Nucleosome dyad is indicated by dashed line; SHL for top turn of DNA indicated by italic numerals. (**C** and **D**) The 90°-rotated views showing crosslinking sites and conformations of the H4 and H4' tails, respectively. Crosslinked sites unaffected or affected by HMGN1 indicated by red or cyan, respectively, site of crosslinker attachment (L10C) indicated by the space-filling residue in the tail domain and green arrow.

ing to nucleosomes in solution (8). We found that formation of covalently crosslinked H1-DNA species, reflecting formation of the H1–nucleosome complex in solution, was unaffected by HMGN1 or 2, even when present at a 30-fold excess (Figure 4). Moreover, single-nucleotide mapping showed that structure-specific interactions between points on the nucleosome surface and two sites within the GH1 are maintained upon association of HMGN2 with H1-bound nucleosomes (Figure 5). These data suggest that the mechanism by which HMGN1 and 2 counteract H1-dependent stabilization of higher order chromatin structures does not rely on simple competition for H1 binding or disruption of H1-globular domain interactions within the nucleosome.

Assuming a more complex mechanism than simple displacement of H1 from nucleosomes, but consistent with the increase in H1 mobility reported previously (30), we considered the possibility that HMGN1 binding alters in some manner interactions that stabilize the binding of H1 within condensed chromatin. The H1 CTD is required for high-affinity binding of H1 to nucleosomes (both *in vitro* and *in vivo*) (14,57) and for stabilization of higher order chromatin structures (3,9,12). Previously we showed that the H1 CTD undergoes a transition from a disordered to a more condensed state upon nucleosome binding, possibly due to adoption of a defined fold or ensemble of folds (14,15,58). Alterations in CTD conformation, either by posttranslational modification or protein interaction, could alter its ability to stabilize higher order chromatin structures. Consistent with this idea, we found the characteristic condensation of the H1 CTD is altered upon binding of HMGN1.

Surprisingly, HMGN1 induces the CTD to adopt a *more* condensed conformation within the nucleosome (Figure 6). This HMGN1-dependent increase in CTD condensation might lower the binding affinity of H1 or reduce potential CTD contacts with linker DNA, effectively loosening chromatin structure. It is important to consider that despite being less abundant overall *in vivo*, HMGN1 protein may be directed to bind concentrated regions of the genome (35). A localized increase in the concentration of HMGN proteins and induction of a more open chromatin structure could lead to more facile exchange of linker histones and local depletion of these proteins from chromatin, in a manner similar to acetylation (59), thereby providing opportunity for the binding of regulatory factors. While understanding how this alteration affects chromatin structure will require additional experimentation, we suggest that such changes may reorient critical H1–CTD interactions with the nucleosome important for stabilizing condensed chromatin. Indeed our data could explain how HMGNs decrease H1 residence time *in vivo* (30), through alteration of H1 CTD interactions, concomitant with the decompaction of chromatin structure (see below).

An alternative, though not mutually exclusive, means of HMGN influence on H1–nucleosome structure and interactions could be mediated through core histone tail domains. A prior report indicates that the H1 binding to nucleosomes can influence core histone tail domain structures and the ability to be modified by acetylases, methylases and kinases (60). Likewise HMGNs have been shown to affect the levels of several histone modifications (61,62) and site directed crosslinking occurs between the N-terminal region of HMGNs and a region spanning residues 20–50 within the histone H3 in nucleosomes (23). In addition, the H3 and H4 tail domains, the binding site for the GH1 and the location of HMGN1/2 association with the nucleosome are in close proximity. Therefore, we hypothesized that HMGNs may directly modulate core histone tail interactions. Using a site-specific crosslinking approach to map interactions of two positions within each of the H3 and H4 N-terminal tail domains with nucleosome DNA to single-base resolution, we found that both histone tails bind DNA at discrete locations, consistent with adoption of defined structures when bound within the nucleosome (Figures 7–9). In particular, crosslinks mapped for the N-terminus of the H4 tail domain are consistent with two predominant conformations of this tail, one of which aligns strikingly well with a tail conformation observed in a crystal structure of the nucleosome core in which these domains are uniquely visualized (Figure 9). Moreover, our data show that the H3 tail domain interacts with both core and linker DNA (Figures 7 and 8), in a manner similar to that predicted by molecular dynamics simulations (55,63).

Importantly, HMGN1 and 2 induce rearrangements of H3 and H4 tail interactions, primarily disrupting core histone tail interactions with linker DNA and with DNA regions closest to the nucleosomal dyad (Figures 7–9). For example, changes in H4 tail interactions are consistent with the HMGNs selectively favoring the H4, rather than the H4' conformation of this tail domain (see Figure 9). In addition Kato *et al.*, ((21) #188] showed that the HMGN2 NBD interacts with the H2A/H2B acid pocket on the nucleosome surface, while we provide evidence (this work) that HMGN1 binds in a similar manner (Figure 2, Supplementary Figures S2 and 3). Thus, the association of HMGNs with nucleosomes would be expected to interfere with internucleosomal interactions between the H4 tail domain and the acidic pocket, thought to be important for formation of condensed chromatin structures [Luger, 1997 #103;Dorigo, 2003 #163]. Likewise, binding of HMGNs disrupts H3 tail interactions in the linker DNA near the edge of nucleosome core DNA and those nearest the dyad axis (Figures 7 and 8). Thus, our data indicate that HMGNs reorient H3 tail contacts to more internal sites within the nucleosome, thereby potentially altering linker DNA trajectory (Figure 10). The notion that HMGNs affect core histone tails is supported by a considerable number of reports that in both *in vivo* and *in vitro* assays showing that HMGN proteins modulate the level of various core histone modifications in a variant-specific manner (64).

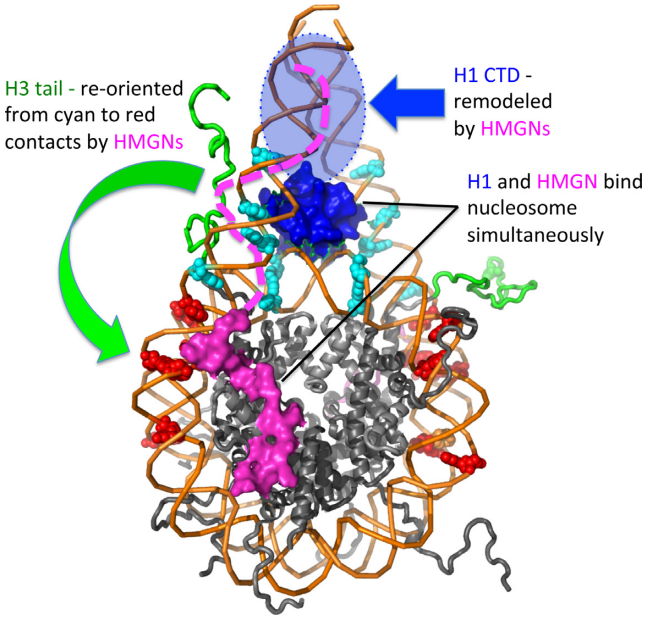

Figure 10. Model of HMGN1/2 and H1 interaction with the nucleosome. Model shows core histones (gray cartoons), DNA (orange ribbon representation), HMGN2 nucleosome binding domain (magenta space-fill), HMGN2 regulatory domain (broken magenta line), GH1 (Bednar *et al.*, (8)) (blue space fill) and the H1 CTD (blue transparent oval with dotted line). The H3 tail domain is colored green, show as in Figure 7, and sites of H3 tail crosslinking summarized from Figures 7 and 8. Those diminished by HMGN1/2 binding are indicated by cyan space-filling bases, those unaffected by HMGNs are red space-filling bases. The direction of reorientation of the H3 tail is indicated.

HMGN-dependent changes in histone tail interactions could facilitate changes in linker DNA trajectory or internucleosome interactions, which, in conjunction with explicit alteration of H1 CTD structure could tip the balance of interactions to favor a less condensed chromatin structure. Alternatively, the effect of HMGNs on the H1 CTD could be indirect, through alteration of linker DNA trajectories (58). Regardless, our data is consistent with observations that elevation of HMGN proteins within cells elevates the rate of exchange of H1.0 within nuclei, in a manner dependent on the ability of HMGNs to bind to nucleosomes (30)

as HMGN-induced rearrangements of core and linker histone tail interactions leads to a less condensed chromatin structure in which H1 exchange would be more facile (59).

In vivo, linker histone mediated chromatin compaction plays an important role in chromatin regulation, impinging on several nuclear processes. Here we provide evidence that HMGNs mitigate H1-dependent self-association of nucleosome arrays, suggesting that HMGN1 and 2 selectively impact long-range inter-nucleosome interactions mediated by both core and linker histone tail domains, but not short-range inter-nucleosome contacts that direct array folding. Thus, our data indicate HMGNs induce an opening of chromatin via directed alteration of core histone tail domains and changes in H1 interactions. The latter could further lead to more rapid exchange of H1 at gene regulatory sites where concentrated HMGN binding occurs in the genome (30,35,36).

SUPPLEMENTARY DATA

Supplementary Data are available at NAR Online.

ACKNOWLEDGEMENTS

We thank Dr Yawen Bai, National Cancer Institute, National Institutes of Health for providing the coordinates for the HMGN2 NBD-nucleosome core model used to create Figure 10.

FUNDING

National Institutes of Health (NIH) [GM052426 to J.J.H.]; Center for Cancer Research, the Intramural Research Program of the National Cancer Institute, National Institutes of Health [ZIA BC 011154 to M.B.]; NIH Training Grant [T32GM068411 to A.R.C., K.J.M.]. Funding for open access charge: NIH [GM02426].
Conflict of interest statement. None declared.

REFERENCES

1. Pepenella,S., Murphy,K.J. and Hayes,J.J. (2014) Intra- and inter-nucleosome interactions of the core histone tail domains in higher-order chromatin structure. *Chromosoma*, **123**, 3–13.
2. Maeshima,K., Rogge,R., Tamura,S., Joti,Y., Hikima,T., Szerlong,H., Krause,C., Herman,J., Seidel,E., DeLuca,J. *et al.* (2016) Nucleosomal arrays self-assemble into supramolecular globular structures lacking 30-nm fibers. *EMBO J.*, **35**, 1115–1132.
3. Carruthers,L.M., Bednar,J., Woodcock,C.L. and Hansen,J.C. (1998) Linker histones stabilize the intrinsic salt-dependent folding of nucleosomal arrays: mechanistic ramifications for higher-order chromatin folding. *Biochemistry*, **37**, 14776–14787.
4. Grigoryev,S.A., Bascom,G., Buckwalter,J.M., Schubert,M.B., Woodcock,C.L. and Schlick,T. (2016) Hierarchical looping of zigzag nucleosome chains in metaphase chromosomes. *Proc. Natl. Acad. Sci. U.S.A.*, **113**, 1238–1243.
5. Syed,S.H., Goutte-Gattat,D., Becker,N., Meyer,S., Shukla,M.S., Hayes,J.J., Everaers,R., Angelov,D., Bednar,J. and Dimitrov,S. (2010) Single-base resolution mapping of H1-nucleosome interactions and 3D organization of the nucleosome. *Proc. Natl. Acad. Sci. U.S.A.*, **107**, 9620–9625.
6. Zhou,B.R., Jiang,J., Feng,H., Ghirlando,R., Xiao,T.S. and Bai,Y. (2015) Structural mechanisms of nucleosome recognition by linker histones. *Mol. Cell*, **59**, 628–638.
7. Cutter,A.R. and Hayes,J.J. (2016) Linker histones: novel insights into structure-specific recognition of the nucleosome. *Biochem. Cell Biol.*, **95**, 171–178.
8. Bednar,J., Garcia-Saez,I., Ramachandran,B., Cutter,A.R., Papai,G., Reymer,A., Syed,S.H., Lone,I.N., Tonchev,O., Crucifix,C. *et al.* (2017) Structure and dyamics of a 197 base-pair nucleosome in complex wth histone H1. *Mol. Cell*, **66**, 384–397.
9. Allan,J., Mitchell,T., Harborne,N., Bohm,L. and Crane-Robinson,C. (1986) Roles of H1 domains in determining higher order chromatin structure and H1 location. *J. Mol. Biol.*, **187**, 591–601.
10. Clark,D.J. and Kimura,T. (1990) Electrostatic mechanism of chromatin folding. *J. Mol. Biol.*, **211**, 883–896.
11. Cutter,A.R. and Hayes,J.J. (2015) A brief review of nucleosome structure. *FEBS Lett.*, **589**, 2914–2922.
12. Lu,X. and Hansen,J.C. (2004) Identification of specific functional subdomains within the linker histone H10 C-terminal domain. *J. Biol. Chem.*, **279**, 8701–8707.
13. Hansen,J.C., Lu,X., Ross,E.D. and Woody,R.W. (2006) Intrinsic protein disorder, amino acid composition, and histone terminal domains. *J. Biol. Chem.*, **281**, 1853–1856.
14. Caterino,T.L., Fang,H. and Hayes,J.J. (2011) Nucleosome linker DNA contacts and induces specific folding of the intrinsically disordered H1 carboxyl-terminal domain. *Mol. Cell. Biol.*, **31**, 2341–2348.
15. Fang,H., Clark,D.J. and Hayes,J.J. (2012) DNA and nucleosomes direct distinct folding of a linker histone H1 C-terminal domain. *Nucleic Acids Res.*, **40**, 1475–1484.
16. Albright,S.C., Wiseman,J.M., Lange,R.A. and Garrard,W.T. (1980) Subunit structures of different electrophoretic forms of nucleosomes. *J. Biol. Chem.*, **255**, 3673–3684.
17. Sandeen,G., Wood,W. and Felsenfeld,G. (1980) The interaction of high moblility proteins HMG-14 and 17 with nucleosomes. *Nucleic Acids Res.*, **8**, 3757–3778.
18. Crippa,M.P., Alfonso,P.J. and Bustin,M. (1992) Nucleosome core binding region of chromosomal protein HMG-17 acts as an independent functional domain. *J. Mol. Biol.*, **228**, 442–449.
19. Ueda,T., Catez,F., Gerlitz,G. and Bustin,M. (2008) Delineation of the protein module that anchors HMGN proteins to nucleosomes in the chromatin of living cells. *Mol. Cell. Biol.*, **28**, 2872–2883.
20. Alfonso,P.J., Crippa,M.P., Hayes,J.J. and Bustin,M. (1994) The footprint of chromosomal-proteins Hmg-14 and Hmg-17 on chromatin subunits. *J. Mol. Biol.*, **236**, 189–198.
21. Kato,H., van Ingen,H., Zhou,B.R., Feng,H., Bustin,M., Kay,L.E. and Bai,Y. (2011) Architecture of the high mobility group nucleosomal protein 2-nucleosome complex as revealed by methyl-based NMR. *Proc. Natl. Acad. Sci. U.S.A.*, **108**, 12283–12288.
22. Brawley,J.V. and Martinson,H.G. (1992) HMG proteins 14 and 17 become cross-linked to the globular domain of histone H3 near the nucleosome core particle dyad. *Biochemistry*, **31**, 364–370.
23. Trieschmann,L., Martin,B. and Bustin,M. (1998) The chromatin unfolding domain of chromosomal protein HMG-14 targets the N-terminal tail of histone H3 in nucleosomes. *Proc. Natl. Acad. Sci. U.S.A.*, **95**, 5468–5473.
24. Trieschmann,L., Alfonso,P.J., Crippa,M.P., Wolffe,A.P. and Bustin,M. (1995) Incorporation of chromosomal proteins HMG-14/HMG-17 into nascent nucleosomes induces an extended chromatin conformation and enhances the utilization of active transcription complexes. *EMBO J.*, **14**, 1478–1489.
25. Kugler,J.E., Deng,T. and Bustin,M. (2012) The HMGN family of chromatin-binding proteins: dynamic modulators of epigenetic processes. *Biochim. Biophys. Acta*, **1819**, 652–656.
26. Ding,H.F., Rimsky,S., Batson,S.C., Bustin,M. and Hansen,U. (1994) Stimulation of RNA polymerase II elongation by chromosomal protein HMG-14. *Science*, **265**, 796–799.
27. Vestner,B., Bustin,M. and Gruss,C. (1998) Stimulation of replication efficiency of a chromatin template by chromosomal protein HMG-17. *J. Biol. Chem.*, **273**, 9409–9414.
28. Birger,Y., West,K.L., Postnikov,Y.V., Lim,J.H., Furusawa,T., Wagner,J.P., Laufer,C.S., Kraemer,K.H. and Bustin,M. (2003) Chromosomal protein HMGN1 enhances the rate of DNA repair in chromatin. *EMBO J.*, **22**, 1665–1675.
29. Postnikov,Y.V. and Bustin,M. (2016) Functional interplay between histone H1 and HMG proteins in chromatin. *Biochim. Biophys. Acta*, **1859**, 462–467.

30. Catez,F., Brown,D.T., Misteli,T. and Bustin,M. (2002) Competition between histone H1 and HMGN proteins for chromatin binding sites. *EMBO Rep.*, **3**, 760–766.
31. Ding,H.F., Bustin,M. and Hansen,U. (1997) Alleviation of histone H1-mediated transcriptional repression and chromatin compaction by the acidic activation region in chromosomal protein HMG-14. *Mol. Cell. Biol.*, **17**, 5843–5855.
32. Graziano,V. and Ramakrishnan,V. (1990) Interaction of HMG14 with chromatin. *J. Mol. Biol.*, **214**, 897–910.
33. Shick,V.V., Belyavsky,A.V. and Mirzabekov,A.D. (1985) Primary organization of nucleosomes. Interaction of non-histone high mobility group proteins 14 and 17 with nucleosomes, as revealed by DNA-protein crosslinking and immunoaffinity isolation. *J. Mol. Biol.*, **185**, 329–339.
34. Woodcock,C.L., Skoultchi,A.I. and Fan,Y. (2006) Role of linker histone in chromatin structure and function: H1 stoichiometry and nucleosome repeat length. *Chromosome Res.*, **14**, 17–25.
35. Cuddapah,S., Schones,D.E., Cui,K., Roh,T.Y., Barski,A., Wei,G., Rochman,M., Bustin,M. and Zhao,K. (2011) Genomic profiling of HMGN1 reveals an association with chromatin at regulatory regions. *Mol. Cell. Biol.*, **31**, 700–709.
36. Deng,T., Zhu,Z.I., Zhang,S., Postnikov,Y., Huang,D., Horsch,M., Furusawa,T., Beckers,J., Rozman,J., Klingenspor,M. *et al.* (2015) Functional compensation among HMGN variants modulates the DNase I hypersensitive sites at enhancers. *Genome Res.*, **25**, 1295–1308.
37. Deng,T., Zhu,Z.I., Zhang,S., Leng,F., Cherukuri,S., Hansen,L., Marino-Ramirez,L., Meshorer,E., Landsman,D. and Bustin,M. (2013) HMGN1 modulates nucleosome occupancy and DNase I hypersensitivity at the CpG island promoters of embryonic stem cells. *Mol. Cell. Biol.*, **33**, 3377–3389.
38. Hill,D.A., Peterson,C.L. and Imbalzano,A.N. (2005) Effects of HMGN1 on chromatin structure and SWI/SNF-mediated chromatin remodeling. *J. Biol. Chem.*, **280**, 41777–41783.
39. Rochman,M., Postnikov,Y., Correll,S., Malicet,C., Wincovitch,S., Karpova,T.S., McNally,J.G., Wu,X., Bubunenko,N.A., Grigoryev,S. *et al.* (2009) The interaction of NSBP1/HMGN5 with nucleosomes in euchromatin counteracts linker histone-mediated chromatin compaction and modulates transcription. *Mol. Cell*, **35**, 642–656.
40. Allahverdi,A., Yang,R., Korolev,N., Fan,Y., Davey,C.A., Liu,C.F. and Nordenskiold,L. (2011) The effects of histone H4 tail acetylations on cation-induced chromatin folding and self-association. *Nucleic Acids Res.*, **39**, 1680–1691.
41. Pepenella,S., Murphy,K.J. and Hayes,J.J. (2014) A distinct switch in interactions of the histone H4 tail domain upon salt-dependent folding of nucleosome arrays. *J. Biol. Chem.*, **289**, 27342–27351.
42. Wang,X. and Hayes,J.J. (2008) Acetylation mimics within individual core histone tail domains indicate distinct roles in regulating the stability of higher-order chromatin structure. *Mol. Cell. Biol.*, **28**, 227–236.
43. Lim,J.H., Catez,F., Birger,Y., Postnikov,Y.V. and Bustin,M. (2004) Preparation and functional analysis of HMGN proteins. *Method Enzymol.*, **375**, 323–342.
44. Chakravarthy,S., Park,Y.J., Chodaparambil,J., Edayathumangalam,R.S. and Luger,K. (2005) Structure and dynamic properties of nucleosome core particles. *FEBS Lett.*, **579**, 895–898.
45. Kan,P.Y., Caterino,T.L. and Hayes,J.J. (2009) The H4 tail domain participates in intra- and internucleosome interactions with protein and DNA during folding and oligomerization of nucleosome arrays. *Mol. Cell. Biol.*, **29**, 538–546.
46. Davey,C.A., Sargent,D.F., Luger,K., Maeder,A.W. and Richmond,T.J. (2002) Solvent mediated interactions in the structure of the nucleosome core particle at 1.9 a resolution. *J. Mol. Biol.*, **319**, 1097–1113.
47. Schauwecker,S.M., Kim,J.J., Licht,J.D. and Clevenger,C.V. (2017) Histone H1 and chromosomal protein HMGN2 regulate prolactin-induced STAT5 transcription factor recruitment and function in breast cancer cells. *J. Biol. Chem.*, **292**, 2237–2254.
48. Schwarz,P.M., Felthauser,A., Fletcher,T.M. and Hansen,J.C. (1996) Reversible oligonucleosome self-association: dependence on divalent cations and core histone tail domains. *Biochemistry*, **35**, 4009–4015.
49. Hansen,J.C. (2002) Conformational dynamics of the chromatin fiber in solution: determinants, mechanisms, and functions. *Annu. Rev. Biophys. Biomol. Struct.*, **31**, 361–392.
50. Postnikov,Y.V., Trieschmann,L., Rickers,A. and Bustin,M. (1995) Homodimers of chromosomal proteins HMG-14 and HMG-17 in nucleosome cores. *J. Mol. Biol.*, **252**, 423–432.
51. Barbera,A.J., Chodaparambil,J.V., Kelley-Clarke,B., Joukov,V., Walter,J.C., Luger,K. and Kaye,K.M. (2006) The nucleosomal surface as a docking station for Kaposi's sarcoma herpesvirus LANA. *Science*, **311**, 856–861.
52. Chodaparambil,J.V., Barbera,A.J., Lu,X., Kaye,K.M., Hansen,J.C. and Luger,K. (2007) A charged and contoured surface on the nucleosome regulates chromatin compaction. *Nat. Struct. Mol. Biol.*, **14**, 1105–1107.
53. Ueda,T., Catez,F., Gerlitz,G. and Bustin,M. (2008) Delineation of the protein module that anchors HMGN proteins to nucleosomes in the chromatin of living cells. *Mol. Cell. Biol.*, **28**, 2872–2883.
54. Gordon,F., Luger,K. and Hansen,J.C. (2005) The core histone N-terminal tail domains function independently and additively during salt-dependent oligomerization of nucleosomal arrays. *J. Biol. Chem.*, **280**, 33701–33706.
55. Li,Z. and Kono,H. (2016) Distinct Roles of Histone H3 and H2A Tails in Nucleosome Stability. *Sci. Rep.*, **6**, 31437.
56. Hansen,J.C. (2002) Conformational dynamics of the chromatin fiber in solution: determinants, mechanisms, and functions. *Annu. Rev. Bioph. Biom.*, **31**, 361–392.
57. Hendzel,M.J., Lever,M.A., Crawford,E. and Th'ng,J.P. (2004) The C-terminal domain is the primary determinant of histone H1 binding to chromatin in vivo. *J. Biol. Chem.*, **279**, 20028–20034.
58. Fang,H., Wei,S., Lee,T.H. and Hayes,J.J. (2016) Chromatin structure-dependent conformations of the H1 CTD. *Nucleic Acids Res.*, **44**, 9131–9141.
59. Perry,C.A. and Annunziato,A.T. (1989) Influence of histone acetylation on the solubility, H1 content and DNase I sensitivity of newly assembled chromatin. *Nucleic Acids Res.*, **17**, 4275–4291.
60. Stutzer,A., Liokatis,S., Kiesel,A., Schwarzer,D., Sprangers,R., Soding,J., Selenko,P. and Fischle,W. (2016) Modulations of DNA contacts by linker histones and post-translational modifications determine the mobility and modifiability of nucleosomal H3 tails. *Mol. Cell*, **61**, 247–259.
61. Lim,J.H., Catez,F., Birger,Y., West,K.L., Prymakowska-Bosak,M., Postnikov,Y.V. and Bustin,M. (2004) Chromosomal protein HMGN1 modulates histone H3 phosphorylation. *Mol. Cell*, **15**, 573–584.
62. Lim,J.H., West,K.L., Rubinstein,Y., Bergel,M., Postnikov,Y.V. and Bustin,M. (2005) Chromosomal protein HMGN1 enhances the acetylation of lysine 14 in histone H3. *EMBO J.*, **24**, 3038–3048.
63. Shaytan,A.K., Armeev,G.A., Goncearenco,A., Zhurkin,V.B., Landsman,D. and Panchenko,A.R. (2016) Coupling between histone conformations and DNA geometry in nucleosomes on a microsecond timescale: atomistic insights into nucleosome functions. *J. Mol. Biol.*, **428**, 221–237.
64. Postnikov,Y. and Bustin,M. (2010) Regulation of chromatin structure and function By HMGN proteins. *Biochim. Biophys. Acta*, **1799**, 62–68.